Bridge Maintenance, Safety, Management, Resilience and Sustainability – Biondini & Frangopol (Eds)
© 2012 Taylor & Francis Group, London, ISBN 978-0-415-62124-3

Expected seismic performance of irregular isolated bridges

J.M. Jara, M. Jara & B.A. Olmos
Civil Engineering School, Universidad Michoacana de San Nicolás de Hidalgo, Morelia, Michoacán, México

D. Villanueva
Civil Engineering School, Universidad de Sonora,Hermosillo, Sonora, México

H. Varum
Department of Civil Engineering, Universidade de Aveiro, Aveiro, Portugal

ABSTRACT: Bridge structures are usually built on irregular topographical surfaces which create substructures with pier heights of different lengths. Three height irregularity types of typical RC medium length bridges are analyzed aimed at determining the best strength and stiffness parameters of an isolation system. The models were located in a high seismicity zone of Mexico. The isolation system is composed by lead rubber bearings (LRB) located on each pile and abutment. The bridge and isolation parameters conducted to the nonlinear time history analysis (NLTHA) of 169 models. Ten seismic records representative of the subduction zone in the Pacific Coast in Mexico were chosen to carry out the study. The maximum drift pier demands, bending moments and shear forces were analyzed to identify the best isolation properties for improving the bridges' structural behavior, specially focused on looking for avoiding irregularity concentrations of shear forces on piers. Additionally, the seismic response of the bridges supported on traditional neoprene bearings was carried out.

1 INTRODUCTION

Many seismic bridge damages in different countries have been identified with force demand concentrations on certain piers of substructures composed by piers with different lengths which conduct to strong lateral stiffness irregularities. This study was motivated by the increasing use of isolation systems in bridges with these characteristics and the lack of studies quantifying the influence of the isolation parameters on the seismic response of bridges with height irregularities. Bridges closely located to active seismic sources are very attractive to incorporate seismic isolation systems, mainly due to the high seismic activity and the typical frequency content of the accelerograms recorded in these areas.

Prestressed concrete beams, frequently AASHTO types, compose the typical superstructure for medium length RC bridges or steel girders supported on neoprene bearings. Piers and abutments with one or more RC columns usually form the substructures.

This study presents the effect of the strength and stiffness isolation properties on the seismic response of irregular medium length RC bridges. A parametric study is conducted to investigate the contribution of the isolation parameters on the seismic response of three typologies of irregular bridges. The models were subjected to ten scaled seismic records recorded close to the subduction zone of the Pacific Coast in Mexico. A total of 1690 3D nonlinear time history analysis in each direction of the bridge models were processed.

2 BRIDGE MODELS

2.1 *Irregularity type 1*

The selection of the bridge parameters intends to characterize typical schemes of variations in pier heights representing a large number of medium length isolated bridges. The substructure irregularity was considered by using a five span simple supported bridge with three pier height configurations. Figure 1 shows the first model with two central piers of the same length and the other two shorter. The bridge is supported on four piers and two fixed abutments. The superstructure in all models remains with the same geometrical and mechanical characteristics. As shown in figure 1, the bridge is composed by five 30 meters long spans.

Using this structural irregularity type, four bridge models were created varying the pier heights (table 1). Model 1 is the regular bridge model whereas model 4 is the model with more pronounced difference between the central and lateral pier heights. The last column of the table displays the ratio between the pier heights.

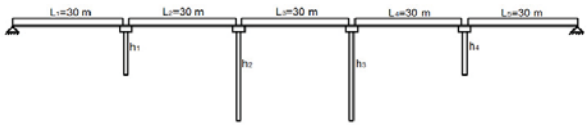

Figure 1. Bridge model with irregularity type I.

Table 1 Pier heights of the type I bridge models.

Model	h_1 (m)	h_2 (m)	h_3 (m)	h_4 (m)	h_2/h_1
MODI_1	|5	5	5	5	1.0
MODI_2	5	7.5	7.5	5	1.5
MODI_3	5	10	10	5	2.0
MODI_4	5	15	15	5	3.0

The superstructure transverse section shown in Figure 2 is composed by eight AASHTO Type IV prestressed beams, placed at every 1.3 m, with parapets at both ends. Diaphragms of 0.38 x 0.77 m were also considered in each third and each end of the span. The pier bent consist of four circular columns with diameter in the range of 1.1 m and 1.3 m, as function of the pier height, and the slab deck thickness is of 0.18 m. The prestressed beams were modeled with a concrete compressive strength of f'c = 350 kg/cm^2 and the rest of the structural elements with f'c = 250 kg/cm^2. The beams are simple supported on 41 mm and 57 mm thick laminated elastomeric rubber bearings.

The model characteristics of this type of bridges produce a cantilever behavior of the piers in longitudinal direction and a frame type behavior in transverse direction, characterized by a lateral deformed shape with an inflexion points in columns.

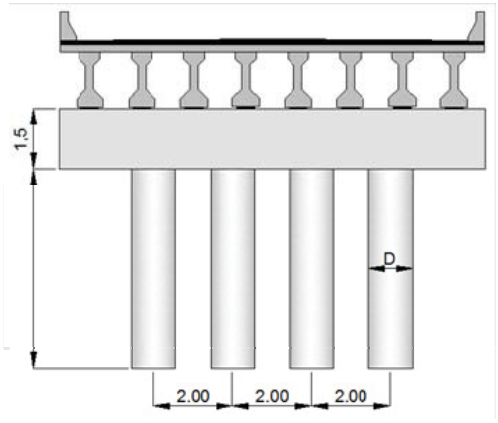

Figure 2. Bridge transverse view.

2.2 *Irregularity type II*

Figure 3 shows the longitudinal view of the bridge model with irregularity type II that is the base of the following five models created. The main irregularity in this model is the height difference among pier 3 and the rest of the bridge piers. Table 2 displays the pier lengths of each model and the height ratio of the pier 3 to pier 1.

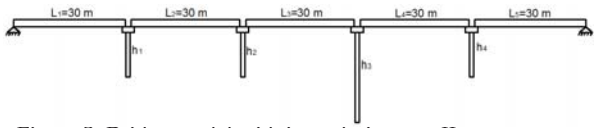

Figure 3. Bridge model with irregularity type II.

Table 2 Pier heights of the type II bridge models.

Model	h_1 (m)	h_2 (m)	h_3 (m)	h_4 (m)	h_3/h_1
MODII_1	|5	5	7.5	5	1.5
MODII_2	5	5	10	5	2.0
MODII_3	5	5	15	5	3.0
MODII_4	7.5	7.5	10	7.5	1.3
MODII_5	7.5	7.5	15	7.5	2.0

2.3 *Irregularity type III*

Figure 4 displays the last type of bridge irregularity created. In this symmetrical model, the pier heights have increasing length up to the central pier (pier 4). The length of pier 4 is in the range of 10 m to 15 m. Table 3 presents the characteristics of each of the four models considered.

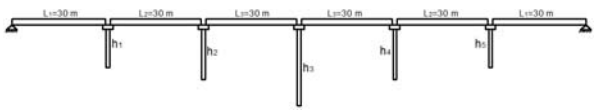

Figure 4. Bridge model with irregularity type III.

Table 3 Pier heights of the type III bridge models.

Modelo	h_1 (m)	h_2 (m)	h_3 (m)	h_4 (m)	h_5 (m)	h_3/h_1
MODIII_1	|5	7.5	10	7.5	5	2.0
MODIII_2	5	7.5	15	7.5	5	3.0
MODIII_3	7.5	10	15	10	7.5	2.0
MODIII_4	5	7.5	10	7.5	7.5	2.0

3 ELASTIC ANALYSIS

3.1 *Design spectrum and modal shapes*

The 13 bridge models were designed using the response spectrum for firm soil (figure 5) of a seismic zone close to the Pacific Coast in Mexico (CFE-2008), and applying the load combinations specified in AASHTO (2005). The live loads used are three types of trucks circulating in Mexico highways, namely: HS-20 (W=32.5 t), T3-S3 (W=48.5 t) and T3-S2-R4 (W=66.5 t).

The columns of the designed models required reinforcement ratios in the range of 1.72% to 2.92%. According to the common practice in this type of bridges, all the columns in each model have the same size and steel reinforcement. Table 4 presents the column diameters, reinforcement ratio, the fundamental periods and the modal movement direction of each model. As observed, there is a narrow interval of period variation in all the bridge types analyzed.

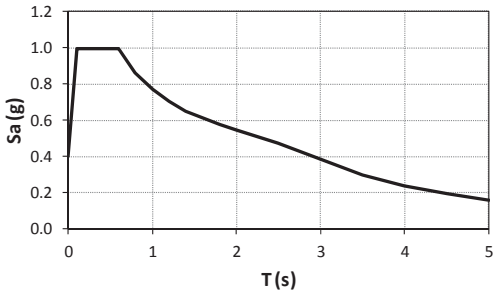

Figure 5. Design spectrum for firm soil.

Table 5 Design results of the bridge models.

Model	Column Diamter (m)	ρ (%)	T (s)	Modal direction
MODI_1	1.1	1.93	0.799	Long
MODI_2	1.1	2.89	0.899	Long
MODI_3	1.3	1.96	0.911	Long
MODI_4	1.3	2.02	1.124	Long
MODII_1	1.1	2.72	0.863	Long
MODII_2	1.3	1.72	0.858	Long
MODII_3	1.3	2.16	0.968	Long
MODII_4	1.3	2.12	0.896	Long
MODII_5	1.3	2.23	1.015	Long
MODIII_1	1.1	2.92	0.989	Long
MODIII_2	1.3	2.22	0.971	Long
MODIII_3	1.3	2.34	1.063	Long
MODIII_4	1.3	1.81	0.881	Long

As an example of the modal shapes, figure 6 shows the modal configuration of the MODI_4 model in the longitudinal and transverse direction.

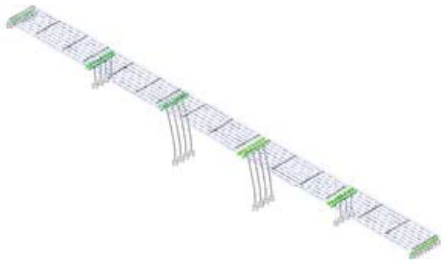

Mode 1, T=1.124 s
(longitudinal)

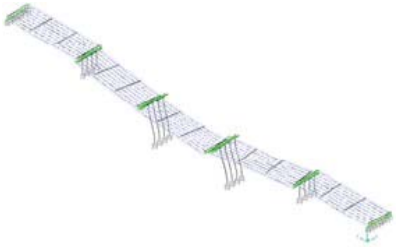

Mode 2, T=0.97 s
(transverse)

Figure 6. First two modal shapes of the MODI_4 model.

4 PARAMETRIC STUDY

For the purposes of this study, four stiffness values of the isolation system were selected aimed at increasing the fundamental period of the models in the range of two to four times. Because of the narrow interval of bridge period variation, the same isolation stiffness was selected for all models. In all cases the post-elastic stiffness was assumed of 10% of the elastic one.

The isolation device strength was also another important parameter studied as well. Initially, the bridge yield forces were obtained by a pushover analysis in longitudinal and transverse directions. Three values of the isolation yield force were analyzed, namely: minimum, medium and maximum. The minimum value was selected to keep the system in the elastic range of behavior for the maximum braking forces of the three load trucks used. The braking forces were assessed using the expression proposed in AASHTO (2005) that, in this case, resulted of 19.95 t for each span of the bridge. This value was in the range of 8% to 10% of the yield shear force on piers in all models. The medium device yield strength was the 50% of the bridge yield force and the maximum device yield force analyzed was the shear yield of the bridge in both directions.

The combination of 13 models with traditional laminated rubber bearings and 13 isolated models with four device stiffness and three device strength values, produced 169 models. The use of ten seismic records leads to 1690 non-linear time history analyses of the bridge models.

4.1 *Seismic records*

The main characteristics of the selected seismic records are: all of them originated in the subduction source in Mexico, they had magnitude greater than 7.0 and they were recorded in hard soil sites. Table 4 shows some parameters of the seismic records used.

Table 4 Characteristics of the seismic records.

Earthquake date	Seismic station	Focal depth (Km)	Epicentral distance (Km)	Magnitude	PGA (cm/s²)
14/03/1979	SICC	28	111.19	7.0	307.22
25/10/1981	APAT	14	135.55	7.3	96.55
	SICC	14	7.927	7.3	265.70
19/09/1985	ZACA	15	81.248	8.1	262.23
	AZIH	15	166.28	8.1	153.93
	PAPN	15	218.38	8.1	154.95
21/09/1985	AZIH	15	46.59	7.6	158.23
	ZACA	15	73.998	7.6	72.73
	PAPN	15	90.04	7.6	242.69
14/09/1995	VIGA	22	62.59	7.2	100.35

The seismic records were scaled to four earthquake return periods according to the study of Jara and Jara (2007). The scaling factor was determined as the ratio of the spectral ordinate of a uniform hazard spectrum corresponding to the bridge fundamental period to the response spectrum of each seismic record for the same period. Figure 7 shows the five uniform hazard response spectrum used in thus study for scaling the seismic signals. The return periods are in the range of 30 years to 2500 years for considering the frequent and rare type earthquakes.

5 SEISMIC ANALYSIS

The non-linear 3D models were created with the Perform 3D software (CSI, 2006) using the same models previously designed with the SAP2000 program (CSI, 2009). The moment-axial load interaction diagrams and moment curvature curves obtained from SAP 2000 were used to define the non-linear properties of the columns in the NLTHA. The girders, diaphragms and cap beams were modeled with beam type elements. In order to consider the distributed mass of the columns, these elements were divided in one meter long sub-elements.

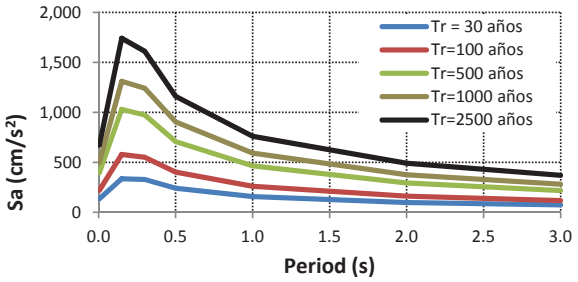

Figure 7. Uniform hazard spectra for five earthquake return periods.

Initially, it was verified that both models (SAP 2000 and Perform 3D) had the same dynamic properties. After that, the Perform 3D models were subjected to the group of seismic records described above. The identification of trends in behavior was conducted by drawing a set of graphs with the seismic response of typical engineering demands as, drift, bending moments, shear forces and ductility against normalized parameters as the stiffness ratio of the seismic isolators to the bridge. It will be only commented in the next paragraphs, because of space limitation, the results of the bridge models with irregularity type I.

5.1 *Results of bridge models with irregularity type I*

Figure 8 shows the ductility demands on the isolators as function of the stiffness ratio (K_{iso}/K_{brd}) for the model MOD1_4 and the maximum isolator yield force in transverse and longitudinal direction. K_{iso} and K_{brd} are the lateral isolator and bridge stiffness, respectively. Each point in the figures represents the isolator ductility for one of the seismic records (ten values for each K_{iso}/K_{brd} ratio). The average ductility values are also presented by a continuous line. As shown, the ductility demand grows with the increase of the K_{iso}/K_{brd} and the maximum ordinate in the graphs is about 2.0 which is a small value for the range of ductility demands the isolators can achieve.

The isolated models with the maximum value of the yield force device capacity led to small ductility demands in the isolation system and the columns undergo inelastic behavior. Hence, in the following paragraphs the results of bridge models with the use of medium and minimum yield shear isolation capacity is presented.

The influence of the isolator yield strength on the device ductility demands can be observed in figure 9. Two extreme cases of K_{iso}/K_{brd} ratios, 3% and 33% in transverse and longitudinal are displayed. It is observed an exponential trend decrease of the ductility demand with the increase of the isolator yield strength. It is evident in this figure the limited ductility demands for the maximum V_{iso}/V_{brd} ratio analyzed.

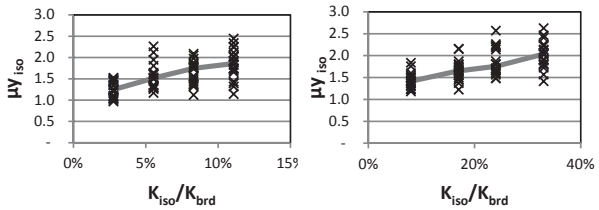

Figure 8. Isolator ductility demands for model MOD1_4 and the maximum value of the device yield force.

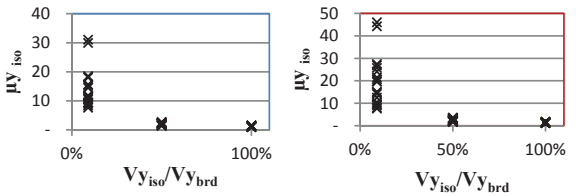

Figure 9. Isolator ductility demands for two stiffness ratio of model MOD1_4. Transverse direction with K_{iso}/K_{brd} = 3% (Left graph) and longitudinl direction with K_{iso}/K_{brd} = 33% (right graph).

For a better visualization of the general trends, the results of the four bridge models derived from model 1 are jointly presented in the figure 10. It shows a group of graphs of the maximum drift demands (θ_{max}) on the short piers in the transverse direction of the bridge model 1. The graphs in the left column display the models with the minimum value of the isolator yield strength and in the right column the results for the medium strength value are presented. In both cases, the horizontal axis displays the isolator to bridge stiffness ratio.

Each graph of the figures also shows with a dashed line the median of the data and with a con-

tinuous horizontal line the model responses on neoprene bearings.

The seismic response of the models MOD1_1 and MOD1_2 are quite similar showing that the increase of the central piers height from 5.0 to 7.5 meters is almost negligible on the drift demands. However, the height increase from 5.0 (MOD1_1) to 15.0 m (MOD1_4) appreciably reduces the drift demands in short piers. Increasing the bridge irregularity makes also important the isolator strength on the pier responses. Hence, the differences between pier drift demands with the minimum and medium isolator strength in MOD1_1 and MOD1_2 are smaller than the differences presented between MOD1_3 and MOD1_4.

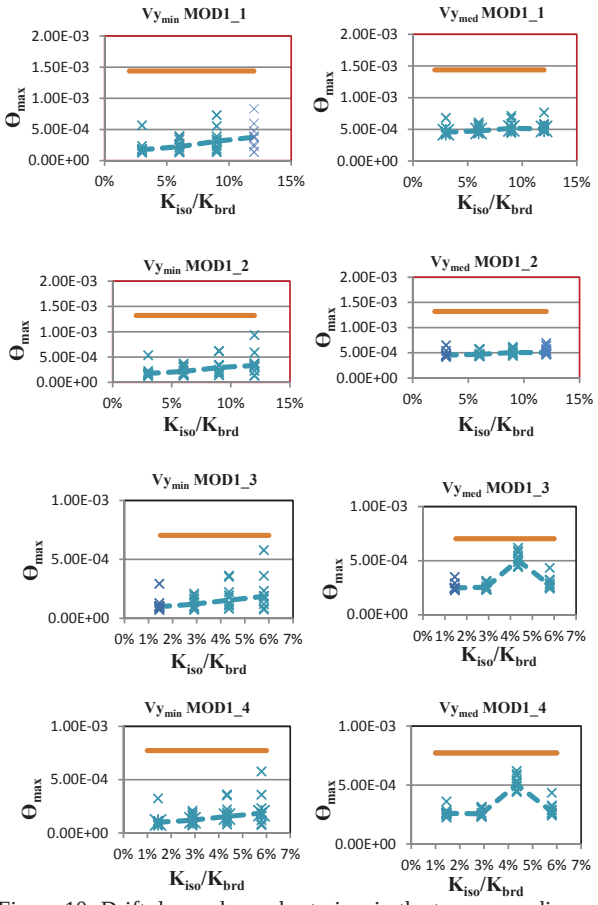

Figure 10. Drift demands on short piers in the transverse direction of the bridge model I.

Bridges supported on piers with different lengths usually presents irregular damage after an earthquake occurrence. Seismic demands concentrations in some piers of traditional supported bridges can be one of the reasons of the damages. Figure 11 shows the ratio of the maximum to the minimum drift value presented in transverse direction of the bridge piers. Again, the horizontal continuous line in each graph is the drift value of the bridge over neoprene bearings.

It is interesting to note that in some of the isolated cases the drift ratio grows instead of being reduced. This specially presented for low stiffness ratios (below 5%). It is also notable the small influence of the isolation on the drift ratio when the minimum isolator yield strength is employed. It is clear from figure 11 that the medium isolator yield strength should be used if we look for more regular behavior among the piers, and the isolation system shows more contribution in the seismic response when the increase of the central pier length (MOD1_3 AND MOD1_4). According to these graphs the drift ratio between two piers can be reduced up to three times the drift ratio on traditional bearings.

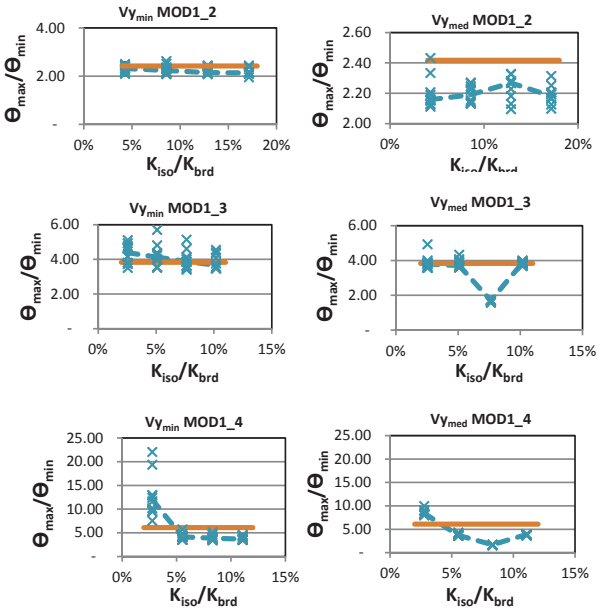

Figure 11. Drift demand ratios between the maximum and the minimum demands on piers in the transverse direction of the bridge.

One relevant engineering parameter to evaluate for understanding the seismic response of the bridges is the shear force demand in piers. Figure 12 presents the maximum shear force demands in longitudinal direction of the short piers for two models of the first type of irregularity analyzed. The inclusion of the isolators conducts to significant shear demand reductions, in particular for the most irregular model (MOD1_4). In these cases, both, the minimum and the medium value of the isolator yield strength produce strong demand reductions.

As expected, there is an increment of the shear force demands on the short piers of the bridge models supported by neoprene pads when the length of the central piers is increased from 5.0 to 15.0 meters. These increases are not reflected on the pier shear forces of the isolated models. Moreover, the medium shear forces of these models are almost unrelated to the isolator-bridge stiffness ratio.

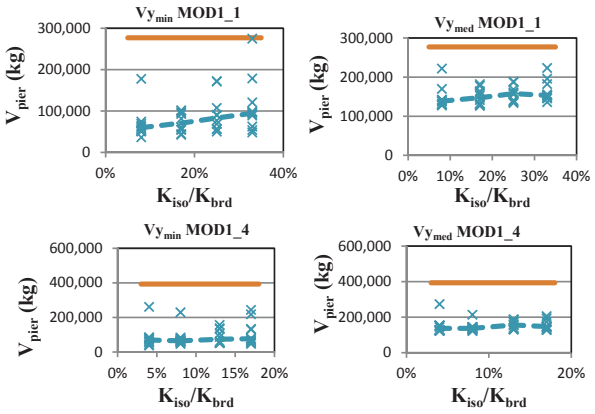

Figure 12. Shear force on short piers in the longitudinal direction of the bridge model I.

It is also remarkable that the shear forces in the isolated models for each device strength remain in similar values when the bridge change from regular one (all piers of 5.0 m height) to an irregular substructure type (two piers 5.0 m height and the other two 15.0 m height).

It is relatively common to find seismic damages in bridges restricted on short piers. These elements are generally stiffer than the long piers demanding large shear forces on them. In order to quantify the influence of the isolation system on the shear demand concentrations, figures 13 and 14 display the pier ratio V_{max}/V_{min} for the longitudinal and transverse direction, respectively of the more irregular bridge model for a type 1 irregularity. V_{max} is the maximum demand in any pier of the bridge and V_{min} the minimum value.

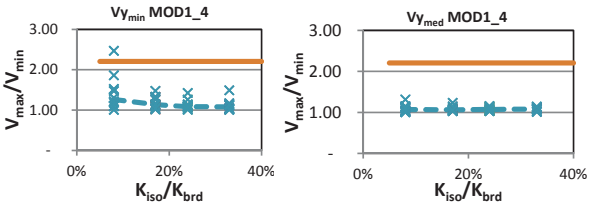

Figure 13. Ratio between the maximum and minimum pier shear forces in longitudinal direction of the bridge model I.

Figure 13 shows that the bridge on neoprene bearings presents shear demands in some pier 2.2 times larger than the demand in other pier of the structure. The isolated model reduces appreciably the V_{max}/V_{min} ratio with all values close to unity. This means that the inclusion of the isolation system in this model conducts to a more regular behavior of the bridge substructure.

In transverse direction, the V_{max}/V_{min} ratio of the non-isolated bridge is reduced to 1.35, showing the benefits of having a frame type substructure (figure 14). Similar to the results in longitudinal direction, the isolated bridge reduced this ratio to values close to unity. In both directions of the isolated models, the shear ratio is almost independent of the isolator-bridge stiffness ratio.

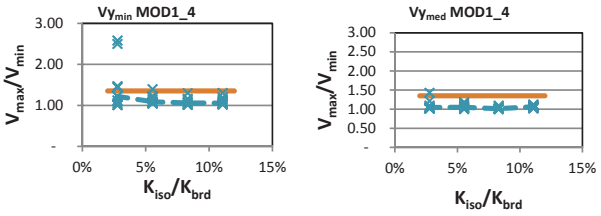

Figure 14. Ratio between the maximum and minimum pier shear forces in transverse direction of the bridge model I.

It is also of interest to determine the isolation influence on the deck movements. Figure 15 shows three graphs of the deck movement in two adjacent spans of the bridge. The first one is the model on neoprene bearings; the second one is the isolated model using the smallest stiffness ratio (K_{iso}/K_{brd}) and the smallest isolator strength (Vy_{min}) and the third graph is again an isolated model with the smallest stiffness ratio and the medium isolator strength (Vy_{med}).

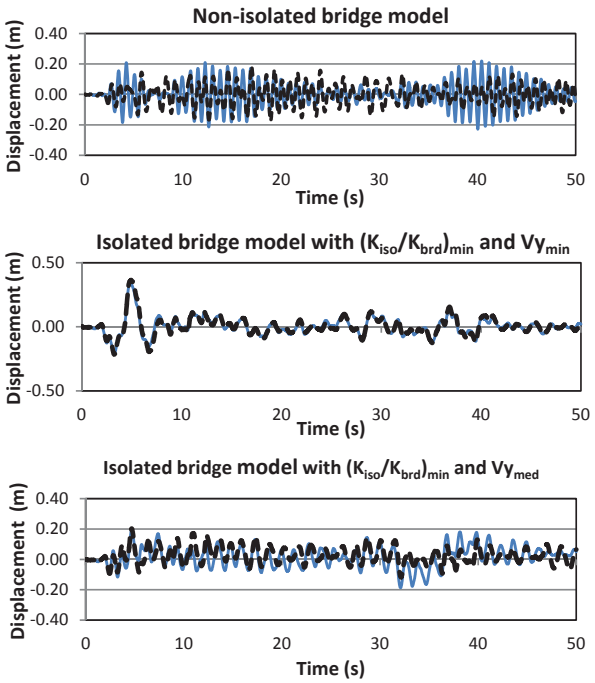

Figure 15. Time history analysis of two adjacent deck spans of three type I bridge models.

The time history analysis of two adjacent deck spans presents out of phase movements in the non-isolated model. The movement amplitudes are considerably different from one span to the other in several intervals of the response record. On the opposite side, the isolated model with the smallest values of the stiffness and strength ratios makes both spans to move in synchrony. However, the use of the mini-

mum isolator strength value yields to the maximum deck displacement demands with the smallest relative displacements between both spans.

The time history analysis of the isolated model employing the medium value of the device yield strength produces displacement demands similar to the case of the non-isolated model but with a more regular behavior. The relative displacements between the decks on the third graph (ordinate difference between solid and dashed lines), are smaller than those values of the non-isolated model (first graph).

Figura 16 displays the pier bending moment demands on the two extreme models analyzed (regular and the most irregular one) in the longitudinal direction of the bridge. Again, the graphs present two isolator strength cases (minimum and medium yield values).

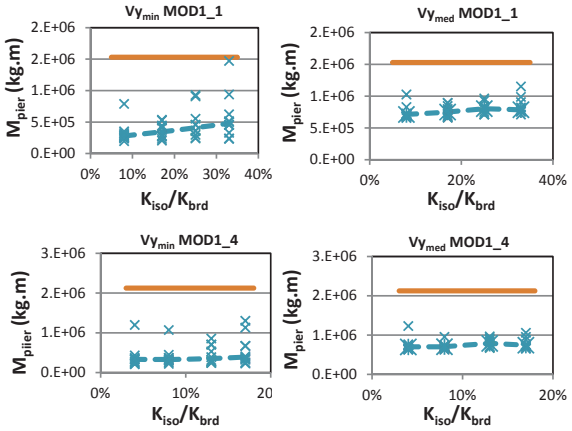

Figure 16. Bending moments demands on short piers in longitudinal direction of the bridge model I.

The bending moment demands in transverse direction are smaller than in longitudinal direction. Figure 17 shows the transverse demands in one column of the short piers in two models of the irregularity type I structures. Again, there is an important response reduction of the bending moment demands for the isolated models.

These figures allow presenting the strong influence of the isolation system for reducing the seismic demands in the short piers. However it is not possible to observe with these graphs the contribution of the isolators for reducing the demand differences between the columns of the bridge. Figure 18 presents the bending moment ratio of the maximum to the minimum columns demands observed during the non-linear time history analysis, in longitudinal direction of the more irregular bridge model analyzed. Both graphs show that in spite of the isolator strength selected (Vy$_{min}$ or Vy$_{med}$), there is a minimum stiffness ratio required to obtain more uniform column demands on the isolated models than the demands on the non-isolated bridge model.

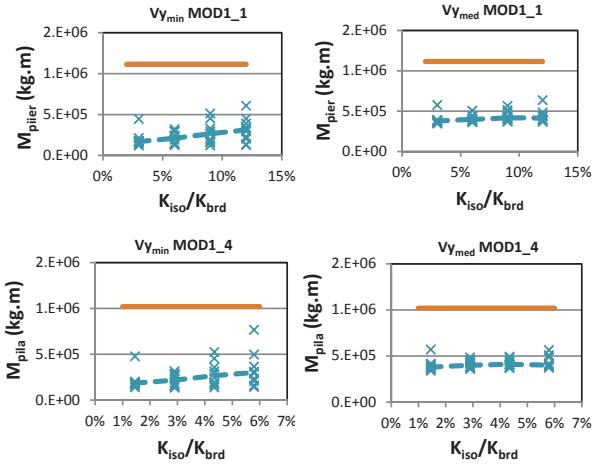

Figure 17. Bending moments demands on short piers in transverse direction of the bridge model I

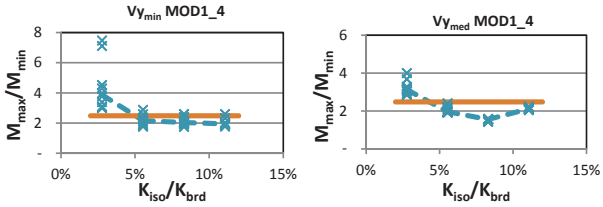

Figure 18. Bending moments demands on short piers in trans

6 CONCLUSIONS

The study presents the results of a research project aimed at assessing the strength and stiffness parameters of an isolation system required to reduce the irregular seismic response of frame type bridges with substructures composed by piers of different heights.

The cantilever behavior in longitudinal direction and the frame type behavior in transverse direction of the piers, produce different parameters of the isolation system. In order to have more uniform seismic response in the substructure, the best ratio between the isolator stiffness and the bridge stiffness in transverse direction was in the range of 6% to 12%. This percentage must be increased to the range of 18% to 28% in the longitudinal direction of the bridge.

The variation of the isolator yield strength showed that a wider range of this parameter can be used to have an appropriate response. The minimum isolator yield value was selected according to the vehicle braking forces and the maximum was limited to the substructure yield force. The isolator to substructure yield strength ratio in the range of 10% to 50% produced the best seismic performance. This parameter should be selected as the smallest ratio possible, considering the isolator ductility capacity.

The outcome of this study can be used to select the strength and stiffness isolator parameters for ir-

regular bridges during the initial phases of the analyses of isolated bridges.

7 ACKNOWLEDGMENTS

This work has been supported by the National Council for Science and Technology (CONACyT) during the sabbatical year of the first author at the University of Aveiro in Portugal, with the grant number 166258 of CONACyT and by the Scientific Research Coordination of the University and Michoacan.

8 REFERENCES

AASHTO 2005. AASHTO LRFD Bridge Design Specifications. *American Association of State Highway and Transportation Officials*. Washington, USA.

CSI 2006. Perform 3D v4.03 Non Linear Analysis and Performance Assessment for 3D structures. *Computers and Structures Inc*. Berkeley, CA, USA.

CSI 2009. SAP2000 v14.0. *Computers and Structures Inc.* Berkeley, CA, USA.

Jara, J.M. & Jara, M. 2007. Sesimic Hazard Assessment in Michoacan. *Internal Technical Report*. Morelia, Mexico.

MOC 2008. Seismic Design of the Civil Works Manual. *Energy Federal Commission*, Mexico (in Spanish).